Enclosure 3

Docket No. PROJ 0782

KHNP Response to RAI 4-7542 on Topical Report "PLUS7 Fuel Design for the APR1400" APR1400-F-M-TR-13001-P Rev.0

June 2014

Non-Proprietary Version

RESPONSE TO REQUEST FOR ADDITIONAL INFORMATION 4-7542

Date of RAI Issued: 05/27/2014
Response Date: 06/26/2014

Question 1

In Sections 1 and 4, discussions on in-pile tests reference Lead Test Assemblies (LTAs) and Commercial Surveillance Assemblies (CSAs). Staff is seeking clarification on the definitions of LTA and CSA. The following additional information is requested:

- Provide a definition of Lead Test Assembly, including any imposed limitations on location, number of LTAs, etc.
- Provide a definition for Commercial Surveillance Assembly, including any imposed limitations on location, number of CSAs, etc.

Response

PLUS7 is an advanced nuclear fuel, jointly developed with Westinghouse to improve fuel performance in both economy and safety. Complete details of the lead test assembly (LTA) and commercial surveillance assembly (CSA) programs to justify PLUS7 for commercial operation are provided in APR1400-F-M-TR-13001-P Rev.0.

In summary, the LTA program was implemented to justify fuel performance for 3 cycles of operation in a nuclear power plant. For this program, four LTAs were irradiated for three cycles from cycle 5 of Ulchin Unit 3. The only limitation imposed on the LTAs was that they operated in non-limiting locations in the core. Results of in-pile tests after each cycle showed that the in-reactor performance of the LTAs was well within their design criteria.

Following the successful LTA program, PLUS7 fuel was put into commercial operation in 2006 starting with cycle 5 of Yonggwang Unit 5. As a follow-up to the LTA program, the CSA program was initiated to evaluate PLUS7 fuel performance in limiting burn-up locations in the core. The CSA program consisted of 1) identifying four PLUS7 fuel assemblies operating in limiting burn-up core locations for two and three cycles of operation, 2) evaluating two of the limiting burn-up fuel assemblies after two cycles of operation and 3) evaluating two other limiting burn-up fuel assemblies after three cycles of operation. The only limitation on location of these fuel assemblies was that they were located in limiting burn-up locations in the core. The results of these evaluations showed that the in-reactor performance of the CSAs was within their design criteria even at the limiting burn-up locations in the core.

Question 2

Section 2.2.2.1 presents the criteria related to the fuel assembly stress limits for normal operation, AOOs, and postulated accidents. Provide additional information regarding the following:

- The minimum ultimate tensile strength at unirradiated conditions (S_u) is listed in the definitions, but is not found in the stress limit equations. How is S_u used in the Plus7 stress limit criteria.
- Is the Sm value, defined by the ASME Section III Stress Intensity for Class 1 Components, for all materials including zirconium alloys? Provide the values used and reference.

Response

The minimum ultimate tensile strength at unirradiated conditions (S_u) is not used directly in the stress limit equations, but it is used to determine S_m' which is the allowable design strength for the postulated accident conditions. The S_m' is a smaller value of 2.4 S_m and 0.7 S_u, which is listed in the definitions of stress limit equation for the postulated accident conditions in section 2.2.2.1 of APR1400-F-M-TR-13001-P Rev.0.

According to the ASME Section III, the S_m, defined by the ASME Section II, Part D, is used for all materials including zirconium alloys. The S_m values for the austenitic steel components are calculated using the values defined in the Table 2A, ASME Section II, Part D and the S_m values for the ZIRLO components are calculated as follows:

- *Two-thirds of the minimum yield strength at temperature*

The S_m values used for the PLUS7 components and the references are in the Table 2-1.

Table 2-1 S_m values for the components at operating temperature

TS

Question 3

In Section 2.2.2.2 it is stated that the evaluation of the rod to top nozzle axial clearance is performed by calculation and confirmed by operating experience. The results of this evaluation are provided in Figure 4-6. The lack of a reference has caused staff to question how the calculation was performed. Provide a detailed description of how the rod to top nozzle axial clearance calculation is performed.

Response

In Figure 4-6 of APR1400-F-M-TR-13001-P Rev.0, the data indicate the rod to top nozzle axial clearances measured for the PLUS7 lead test assemblies (LTAs) and commercial surveillance assemblies (CSAs) during the pool side examinations (PSEs), and "95% lower prediction bound" is a line drawn by processing the measured data statistically.

The rod to top nozzle axial clearance was calculated considering dimensions of the PLUS7 components, thermal expansions, and irradiation growths of fuel rod and fuel assembly by the following equation:

- *Rod to top nozzle axial clearance = $C - E + I_{GT} - I_{FR}$*

  Where, C: Rod to top nozzle axial clearance (as-built),
  E: Thermal expansion difference between fuel rod and guide tube,
  I_{GT}: Irradiation growth of guide tube,
  I_{FR}: Irradiation growth of fuel rod.

The calculated minimum clearance by using the above equation is [
$]^{TS}$.

Question 4

In Section 2.2.2.3, hydraulic stability is partially demonstrated through tests performed in the FACTS loop test facility. The range of flows chosen for the tests has caused staff to question the maximum design flow rate for the PLUS7 fuel assembly.

- What is the maximum design flow rate for the PLUS7 fuel assembly?
- Explain what is meant by "equivalent mechanical design flow in the FACTS test", which was used in Section 2.0 of Appendix A.2.1. How does this value differ from in-reactor design flow?

Response

By considering the limiting reactor vessel flow rate, the total number of fuel assemblies (FAs) in core and total bypass flow, [

]^{TS}.

In addition, the flow in reactor is not equal to that in the fuel assembly compatibility test system (FACTS) due to the difference of FA channel size between the OPR1000 and FACTS facility. Therefore, the flow rate in FACTS was adjusted to be the same flow velocity as the reactor. Considering in-reactor mechanical design flow [ ]^{TS}, the channel size per FA in the OPR1000 and FACTS facility, block area in PLUS7 fuel and bypass flow in PLUS7 fuel, [ ]^{TS}. This is "equivalent mechanical design flow in FACTS."

In summary, [ ]^{TS}. Also, the equivalent mechanical design flow in FACTS was adjusted considering in-reactor mechanical design flow for PLUS7 fuel, the difference of FA channel size between the OPR1000 and FACTS facility, etc.

Note:

TS

Question 5

The stress analyses for the bottom and top nozzles discussed in Sections 2.3.1.2 and 2.3.2.2 are based on an assumed load, which has caused staff to question the basis for the assumed load. Additionally, staff is seeking clarification of the calculation procedure for the stress analyses. Provide the following:

- Explain how the value for the assumed load during postulated accidents is conservative.
- Provide a summary of the calculation procedure for the stress analyses, including the codes utilized for the calculation, imposition of boundary conditions, and how adequate mesh refinement was determined.

Response

Since the load information of postulated accidents at a specific site was not available during the development of the PLUS7 fuel, the load during postulated accidents was conservatively assumed to be [ ]^{TS}. By the comparison between the assumed load and loads during postulated accidents for the NRC DC project (Table 5-1), the assumed load is deemed to be conservative.

Table 5-1 Maximum Axial Loads for PLUS7 Fuel Assembly

TS

The following calculation procedure for the stress analyses is performed sequentially by using the ANSYS version 5.6.2, which consists of assumption, modeling, material properties, applied load and boundary condition, meshing and analysis.

Top nozzle

The PLUS7 top nozzle components, holddown plate and adapter plate, were modeled using three-dimensional solid elements [ ]^{TS} consisting of 10 nodal points per element. The degree of freedom per [ ]^{TS} element nodal point is Ux, Uy, Uz. The special option of ANSYS (called "smart element sizing") was used for meshing the model. The one-eighth model was developed by utilizing symmetry in the geometry and loading conditions. To simplify and conservatively analyze the top nozzle, the chamfers or fillets were not modeled.

- *The assumptions used in this analysis are summarized:*
  - ✓ *Nominal dimensions*
  - ✓ *Material properties at the specific temperature condition*

In case of the holddown plate analysis, the assumed load during postulated accidents was applied as uniformly distributed loads at the interface between the holddown plate outer hub and the colandria tube as shown in Figure 5-1. In order to simulate the contact between spring and holddown plate, the contact area was restrained in the axial direction of the fuel assembly.

In case of the adapter plate analysis, the assumed load during postulated accidents was applied as uniformly distributed loads on the holddown spring seating surface as shown in Figure 5-2. The supported area by guide thimble flange was restrained in the axial direction of the fuel assembly.

Bottom nozzle

The PLUS7 bottom nozzle was modeled using the same three-dimensional solid elements [ ]^{TS} as the top nozzle. The "smart element sizing" option was also used for meshing the model. The one-eighth model was developed by utilizing symmetry in the geometry and loading conditions. To simplify and conservatively analyze the bottom nozzle, the flow hole inlet chamfer on the bottom nozzle plate and the instrument guide were not modeled.

- *The assumptions used in this analysis are summarized:*
  - ✓ *Nominal dimensions except the minimum thickness for the bottom nozzle plate*
  - ✓ *Material properties at the specific temperature condition*

The assumed load during postulated accidents was applied to the bottom nozzle. Uniformly distributed loads were applied to the guide thimble location on the bottom nozzle plate as shown in Figure 5-3. The bottom surface of leg was restrained in the global U_x, U_y, U_z directions.

Meshing

A sensitivity study was performed to determine adequate mesh for stress analysis of the PLUS7 top and bottom nozzles by adjusting the element size.

By comparing P_m+P_b per each element size, adequate mesh size was determined as follows:

- *In case of the holddown plate, the element sizes of [ ]^{TS} were used and mesh was generated using the "smart element sizing" option. The sensitivity study shows that P_m+P_b at each size were within [ ]^{TS} of each other. Therefore, element size for the holddown plate was selected to be [ ]^{TS}.*

- *In case of the adapter plate, the element sizes of [ ]^{TS} were used and mesh was generated using the "smart element sizing" option. The sensitivity study shows that P_m+P_b at each size were within [ ]^{TS} of each other. Therefore, element size for the adapter plate was selected to be [ ]^{TS}.*

- *In case of the bottom nozzle, the element sizes of [ ]^{TS} were used and mesh was generated using the "smart element sizing" option. The sensitivity study shows that P_m+P_b at each size were within [ ]^{TS} of each other. Therefore, element size for the bottom nozzle was selected to be [ ]^{TS}.*

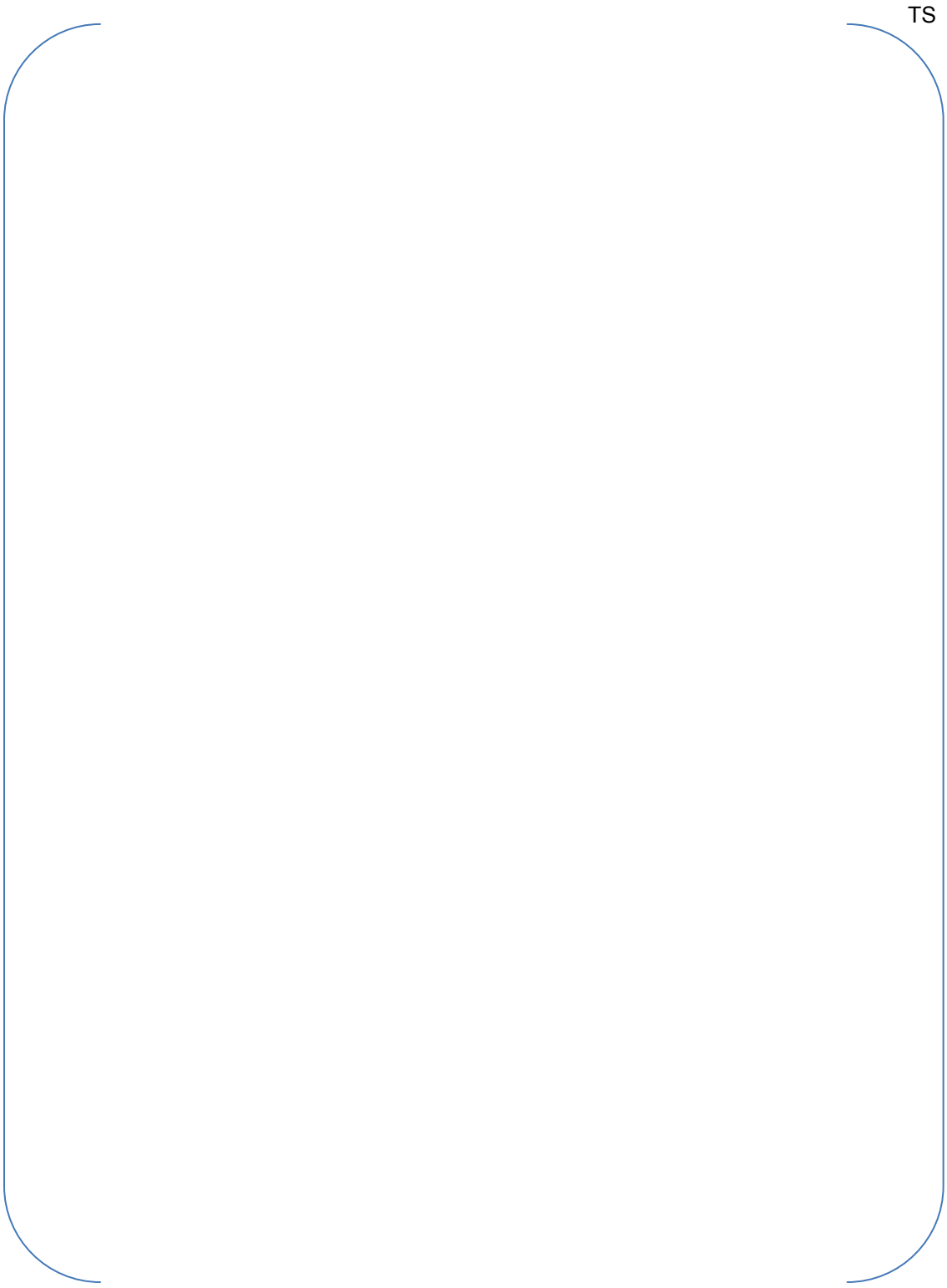

Figure 5-1 Boundary Conditions of Holddown Plate

Figure 5-2 Boundary Conditions of Adapter Plate

Figure 5-3 Boundary Conditions of Bottom Nozzle

Question 6

The proposed oxide limit in Section 3.2.4 of APR1400-F-M-TR-13001-P is 100 μm. Figure 4-44 indicates that cladding with 100 μm of oxide thickness would exceed the 600 ppm hydrogen content limit, which would lead to a loss of ductility. How does the use of a 100 μm oxide thickness limit support the 1% strain criterion?

Response

As proposed in Section 3.2.4 of APR1400-F-M-TR-13001-P Rev.0, the cladding hydrogen is currently limited to 600 ppm on a best estimate basis at end of life to preclude loss of ductility due to hydrogen embrittlement by the formation of zirconium hydride platelets. However, the specific limit value of 600 ppm was not determined by the firm basis on the specified ductility correlation for fuel cladding. It appears that the 600 ppm limit was chosen as a design limit because it was a conservative value for maintaining ductility, and was well above the hydrogen content values that existed when it was selected. The hydrogen-associated effect on ductility is also mainly explained by several combination factors such as temperature, hydride morphology, direction of principal stress, and strain rate, as well as the absolute level of hydrogen contents. Therefore, in consideration of historical determination and related factors, the exceeding a single limiting value of 600 ppm on a best estimate basis needs not to be concerned.

Furthermore, the main reason for the reduction in Zircaloy-4 strain capability is an irradiation hardening effect. The clad hydrogen content plays a lesser role since most of the hydrogen is in solution or precipitates as zirconium hydride platelets which are ductile at normal cladding operating temperatures. Therefore, the hydrogen does not have a significant impact on the cladding ductility at operating temperatures.

In conclusion, ductility is not significantly affected at operating temperatures and not susceptible up to hydrogen levels of 930 ppm shown in Figure 6-1. Therefore, as the 1% strain limit for cladding ductility was introduced to preclude excessive cladding deformation during normal operation and anticipated operational occurrences (AOOs), the 100 μm oxide thickness limit still supports the 1% strain criterion.

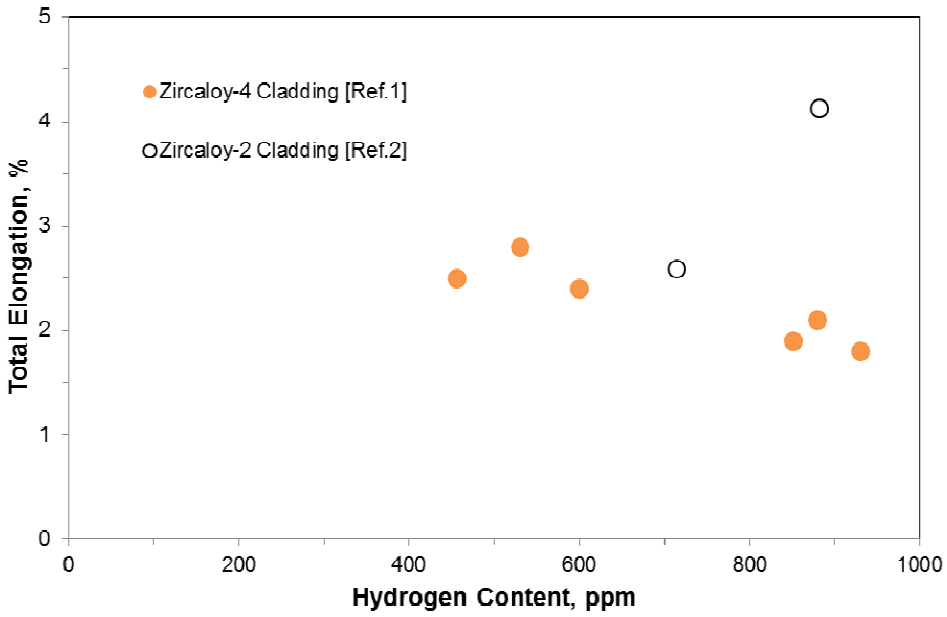

Figure 6-1 Measured Total Elongation vs Hydrogen Content
(Irradiated fuel cladding & Tested at 300℃ or 350℃)

Note: References

[Ref.1] Yagnik S, "Ductility of Zircaloy-4 Fuel Cladding and Guide Tubes at High Fluences," Journal of ASTM International, Vol.2, No.5, May 2005.

[Ref.2] Yagnik S, "Effect of Hydrides on the Mechanical Properties of Zircaloy-2," Orlando, Fl., 2004(b).

Question 7

Section A.2.1 describes the methodology to determine if there are flow induced vibration (FIV) resonances which could lead to fuel failures. It is stated that the vibration spectra is inspected for peaks. What is the criterion for determining if such resonances exist?

Response

The objective of the fuel assembly compatibility test system (FACTS) vibration test is to confirm that the PLUS7 design is not susceptible to high resonance flow-induced assembly vibration over a range of plant operation flow rate. The design acceptance criteria for the fuel assembly (FA) resonant vibration are as follows:

- *No resonant FA vibration phenomena will be observed within the reactor operating flow rate,*
- *The overall vibration amplitude, for frequencies in the range of 0 ~ 100 Hz, will be less than [ ]^{TS} for reactor operating flow rates.*

As a result of the FACTS vibration test for the PLUS7 fuel, there was no indication of abnormal flow induced vibration response throughout the test flow range [ ]^{TS} as shown in Figure A.2.1-2 of APR1400-F-M-TR-13001-P Rev.0. Data in this figure are the maximum vibration amplitude at each flow rate in the range of 0 ~ 100 Hz. Especially, the vibration amplitude of the FA is [ ]^{TS} and the peak is not detected throughout the reactor operating flow range of [ ]^{TS}. Therefore, the vibration characteristics of the PLUS7 fuel were verified through this test. In addition, there has been no issue of vibration on the PLUS7 fuel since the initial commercial supply.

Question 8

The FIV tests presented in Appendix A did not result in fretting wear-induced cladding failure caused by cross-flow or natural harmonics through the full range of flow rates. However, it is not stated that there were no indications of fretting wear associated with FIV. How much wall thinning occurred as a result of FIV and how was this incorporated into the stress analysis?

Response

Fuel rod fretting wear was evaluated through the vibration investigation and pressure drop experimental research (VIPER) long-term wear test and confirmed by the hot cell examination on the PLUS7 lead test assembly (LTA). The VIPER test results are summarized in the Appendix A.2.2 and the results of hot cell examination are described in Section 4.3.1 of APR1400-F-M-TR-13001-P Rev.0.

As a result of the VIPER test, the number of worn-rods and maximum wear depth of the each rod are described in Table A.2.2-2 and Figure A.2.2-1 of APR1400-F-M-TR-13001-P Rev.0, respectively. None of the [ ]^{TS} oxidized rods had measurable wear depth while [ ]^{TS} non-oxidized rods had measurable wear depth as shown in Table A.2.2-2 and Figure A.2.2-1 of APR1400-F-M-TR-13001-P Rev.0. Through the hot cell examination, spring contact area of fuel rod was sliced in 8 pieces with one (1) mm thickness to measure the wear depth. The results of cross section examinations showed that there was no measureable fretting wear depth as described in the Section 4.3.1 of APR1400-F-M-TR-13001-P Rev.0. Therefore, the evaluation shows that the PLUS7 fuel rod would not have fretting wear.

With regard to the stress analysis, fretting on the fuel rod clad surface will not have a significant effect on stresses. There should be only a small dependence of cladding stresses on fretting wear because this type of wear is local at grid contact locations, relatively shallow in depth, and on the clad outer surface, where stresses are lower than in other clad areas. As mentioned above, the flow induced vibration (FIV) test results indicate that there is no measurable wear depth on the surface of the PLUS7 fuel rod. The fretting wear therefore has a very small effect on the cladding stress evaluations. Nevertheless, the PLUS7 clad stress analysis was performed assuming the clad wall thinning effect due to [ ]^{TS} which corresponds to the [ ]^{TS}, and the calculation results show that the stresses in the cladding are within the allowable limits. This is a conservative approach because an actual clad wall thinning occurred by fretting wear is negligible compared to the reduction value assumed in the clad stress analysis.

Question 9

Figure 4-10 presents LTA and CSA predicted oxide thickness versus measured thickness. The staff noted a difference between the prediction accuracy for the LTA data versus the CSA data. While the CSA oxide thickness appears to be typically over predicted, which is conservative, the staff would like to understand the reason for the differences. Please provide a discussion which explains the differences between the CSA and LTA data presented in Figure 4-10 and an explanation of why the CSA oxide thickness appears to be over predicted while the LTA oxide thickness appears to follow a best estimate prediction.

Response

The current ZIRLO corrosion model is based on the [ ]^{TS} corrosion model originally developed for Zircaloy-4 clad. Comparison of the measured cladding oxide thickness on ZIRLO rods to the measured cladding oxide thickness on Zircaloy-4 rods with similar power histories, indicated that the ZIRLO cladding corrosion rate was [ ]^{TS} of the Zircaloy-4 cladding corrosion rate [Ref.1]. Thus, the ZIRLO corrosion model became [ ]^{TS} times the [ ]^{TS} Zircaloy-4 corrosion rate [Ref.1]. The pool side examination (PSE) for the PLUS7 lead test assemblies (LTAs) were conducted in 2007, which reflected the [ ]^{TS} model prediction results. After that, based on the measured data from other domestic plants in addition to the PSE results for the PLUS7 LTAs, KEPCO NF found that the design corrosion model [ ]^{TS} did not accurately predict oxide thickness on the surface of ZIRLO cladding. Thus, the [ ]^{TS} model for ZIRLO cladding was replaced by [ ]^{TS} model which conservatively predicts the oxide thickness for ZIRLO cladding irradiated in domestic plants [Ref.2]. The PSE for the PLUS7 commercial surveillance assemblies (CSAs) were conducted in 2011 and the predicted oxide thickness was calculated using the [ ]^{TS} model.

Additionally, the predicted oxide thickness data for the PLUS7 LTAs were modified based on the [ ]^{TS} model for standard comparison. The modified prediction results in Figure 9-1 conservatively bounds the measured oxide thickness data for the PLUS7 LTAs.

TS

Figure 9-1 Comparison of Measured and Predicted Cladding Oxide Thickness for the PLUS7 LTAs and CSAs

Note: References

[Ref.1] VANTAGE+ Fuel Assembly Report Core Report, WCAP-12610-P-A, April 1995.

[Ref.2] Verification Report on Oxide Thickness Prediction Model of ZIRLO Cladding, KNF-TR-MTL-07002, Rev.0, March 2007.

Question 10

Figure 4-44 contains predicted and measured hydrogen content data for the CO3 LTA. Two of the three data points indicate an under prediction of hydrogen content. Provide predicted hydrogen content data for the Kori Unit 2 and Yonggwang Unit 4 data presented in Figure 4-44.

Response

The predicted hydrogen content data for the Kori Unit 2 and Yonggwang Unit 4 are presented in Figure 10-1. All the available data for the hydrogen content obtained from other domestic plants (Yonggwang Unit 2 & Kori Unit 3) are added to Figure 10-1. Based on this data, the predicted hydrogen contents appear to reasonably follow general trend of measured scattering data.

Figure 10-1 Comparison of Measured and Predicted Hydrogen Content vs Predicted Oxide Thickness